Mon. Not. R. astr. Soc. (1971) **152,** 1–19.

RADIATIVE TRANSFER IN SPHERICALLY SYMMETRIC SYSTEMS. THE CONSERVATIVE GREY CASE

D. G. Hummer and G. B. Rybicki

(Received 1970 December 4)

SUMMARY

A practical computational method is presented for the solution of radiative transfer problems in spherically symmetric systems. This procedure involves iteration on the ' Eddington factor ' $f = K/J$ and is designed to handle the outward peaking of the radiation field in extended spherical systems. Extensive numerical results are obtained and discussed for systems in which $\kappa\rho = r^{-n}$, $0 < r \leqslant R$, for $n = 3/2$, 2 and 3.

1. INTRODUCTION

The purpose of this paper is two-fold: (1) to develop a practical computational procedure for the solution of radiative transfer problems in spherically symmetric systems; and (2) to present and discuss accurate numerical solutions for the simplest spherical analogues of the classical Milne problem in the plane-parallel geometry, that is, an atmosphere of radius R, in radiative equilibrium, with a volume absorption coefficient whose dependence on the radial coordinate r takes the form

$$k(r) \equiv \kappa\rho = \alpha r^{-n}, \quad 0 \leqslant r \leqslant R, \quad (n > 1). \tag{1.1}$$

Problems of this type appear to have first been considered by Kosirev (1934), for $n = 3/2$ and $R = \infty$, and by Chandrasekhar (1934a, b, 1935) for $n = 2$ and 3 with finite values of R. Both Kosirev and Chandrasekhar used variants of the well-known Eddington approximation. Subsequently Chandrasekhar (1945) obtained approximate solutions for cases with $R = \infty$ by a procedure equivalent to retaining the first two terms in a spherical harmonic expansion of the intensity. Wrubel (1949) generalized Chandrasekhar's treatment to account for polarization and Pearce (1967) performed a calculation analogous to Chandrasekhar's for finite spheres with $n = 3/2$ and 2. Wilson & Sen (1965a, b) have also treated the problem with $n = 2$ by a half-range expansion method, again in the second order. However, as Chapman (1966) has emphasized, all of these attempts have ignored a critical feature of these problems, namely that *as r becomes large the intensity I(r) becomes increasingly sharply peaked in the outward radial direction.* Chapman's own solution for $n = 3$ and $R = \infty$, is tolerably accurate and for the first time takes into account the outward peaking of the radiation field. Larson (1969) has obtained approximate solutions of the non-grey problem with $\kappa_\lambda\rho = r^{-3/2}\,\lambda^{-p}$ by arguments similar to those of Chapman. Recently an improved version of Chapman's procedure has been used by Schmid-Burgk (1971 to be published) to obtain what appears to be a very accurate solution for $n = 3$ and $R = \infty$. Finally Cassinelli (1971) has developed a procedure based on the S_n-method of Carlson & Lathrop (1968) for the solution of spherical problems with an arbitrary radial dependence of the opacity; unfortunately this procedure has to be augmented in rather *ad hoc* ways. All of this work,

with the exception of Cassinelli's, depends crucially on the properties of the inverse power opacity laws, in order to evaluate the formal solution, and consequently does not provide a basis for practical work, such as the computation of spherical model atmospheres for certain objects with extended atmospheres.

The method developed here has two principal features: (1) the use of a *cylindrically* symmetric coordinate system which allows the outward peaking to be treated in a natural way and greatly simplifies the numerical evaluation of the formal solution; and (2) iteration on the so-called Eddington factor,

$$f(r) \equiv K(r)/J(r), \tag{1.2}$$

where $J(r)$ and $K(r)$ are the zeroth and second moments of the intensity. The coordinate system, which we refer to as the p–z representation, appears to have been first employed in the evaluation of the formal solution of spherical problems by Kosirev (1934) and Chandrasekhar (1934a, b, 1935), and has recently been employed by Castor (1970) in a study of expanding, spherical envelopes.

The idea of iteration on the ratio of K/J seems to arise from Eddington (1926), who obtained a second approximation for plane-parallel atmospheres. Eddington's treatment is repeated by Woolley & Stibbs (1953). This idea is further referred to by Böhm-Vitense (1963) and by Feautrier (1964b). However, not until the work of Auer & Mihalas (1970) was iteration on the Eddington factor used for practical transfer calculations in plane-parallel geometries. In recent years a variable Eddington factor whose spatial dependence was assumed *a priori* has been used in the solution of radiation hydrodynamics problems in plane, spherical and cylindrical geometries; unfortunately the only readily available reference to this work is that of Pomraning (1969).

In the next section, after a brief review of some of the general features of the solutions we seek, we proceed to develop the iteration procedure for the Eddington factor. Section 3 contains a brief discussion of the computational aspects of the problem. In the final section extensive numerical results are presented for $n = 3/2$, 2 and 3 and general features of the solution are discussed.

2. BASIC RELATIONS

The transfer equation for conservative scattering in a grey spherical atmosphere, as conventionally written in polar coordinates, is

$$\mu \frac{\partial}{\partial r} I(r, \mu) + \frac{1}{r}(1-\mu^2) \frac{\partial}{\partial \mu} I(r, \mu) = -k(r)[I(r, \mu) - J(r)], \tag{2.1}$$

where $k(r)$ represents the volume 'absorption' coefficient $\kappa\rho$, as in equation (1.1) and μ is the cosine of the angle between a radius vector and the direction of propagation of radiation at radius r. Here $J(r)$ is the zeroth moment of the radiation field

$$J(r) \equiv \tfrac{1}{2} \int_{-1}^{1} d\mu I(r, \mu); \tag{2.2}$$

additionally we require the two higher moments

$$H(r) \equiv \tfrac{1}{2} \int_{-1}^{1} d\mu \mu I(r, \mu) \tag{2.3}$$

and

$$K(r) \equiv \tfrac{1}{2}\int_{-1}^{1} d\mu\mu^2 I(r, \mu). \tag{2.4}$$

For opacities of the type given by (1.1), the optical distance from any radius to $r = 0$ is infinite and we may suppose that a point source is located at the origin in precisely the same way as a plane source is located at infinite optical depth in the plane-parallel Milne problem. This point source is assumed to emit L units of energy per unit time. The specification of the problem is completed by requiring that no radiation fall from the outside onto the surface $r = R$.

In the problem as stated two quantities having dimension of length appear, R and $\alpha^{1/n-1}$. We choose the latter as our unit of length, so that (1.1) becomes

$$k(r) = r^{-n}, \quad n > 1. \tag{2.5}$$

With this choice of scale, the mean free path, $k^{-1}(r)$, is equal to the radius at $r = 1$. Then for $r < 1$, the mean free path is smaller than the radius so that the effects of curvature on the radiation field are unimportant, although the r^{-2} dependence of the flux will still play a role; for $r > 1$, the curvature effects are dominant.

By operating on (2.1) with

$$\tfrac{1}{2}\int_{-1}^{1} d\mu \ldots \quad \text{and} \quad \tfrac{1}{2}\int_{-1}^{1} d\mu\mu \ldots,$$

we obtain the moment equations

$$\frac{dH}{dr} + \frac{2}{r} H = 0 \tag{2.6}$$

and

$$\frac{dK}{dr} - \frac{1}{r}[J - 3K] = -k(r)H. \tag{2.7}$$

A solution of (2.6) is

$$H = H_0 r^{-2} \tag{2.8}$$

where H_0 is a constant of integration which has the value $L/(4\pi)^2$ for the point source just described. By introducing the *Eddington factor* defined in equation (1.2) and using (2.8) we can rewrite (2.7) as

$$\frac{d}{dr}(fJ) - \frac{1}{r} J[1 - 3f] = -k(r)H_0 r^{-2}. \tag{2.9}$$

This equation differs from the analogous equation in the plane parallel case in two respects. The second term on the left represents the effects of curvature and becomes negligible for sufficiently small r, while the term on the right represents the spherical dilution of the flux and is important for all radii. It therefore appears that the often-mentioned plane–parallel limit of spherical systems does not, in fact, exist, except in thin spherical shells.

Deep within the atmosphere where the radiation field is essentially isotropic, it is clear from (2.2) and (2.4) that

$$f \cong 1/3, \quad r \ll 1. \tag{2.10}$$

If $f \to 1/3$ faster than $r \to 0$, we see from (2.9) that

$$J \underset{r\to 0}{\sim} -3H_0 \int^{r} dr r^{-2} k(r) \tag{2.11}$$

and if $k(r)$ is given by (2.5),

$$J \underset{r\to 0}{\sim} \frac{3H_0}{n+1} r^{-(n+1)} + \text{constant}. \tag{2.12}$$

For sufficiently small r, the constant in (2.12) is negligible.

On the other hand, if R is large, $I(r, \mu)$ becomes increasingly sharply peaked about $\mu = 1$ as r increases, so that

$$J \cong H \cong K \tag{2.13}$$

and

$$f \cong 1, \quad 1 \ll r \leqslant R. \tag{2.14}$$

A direct consequence of (2.8) and (2.13) is

$$J(r) \sim H_0 r^{-2}. \tag{2.15}$$

For finite R, this result breaks down for $r \simeq R$, although for $R = \infty$ it is a true asymptotic expression. Through his failure to recognize the outward peaking of the radiation field Chandrasekhar (1945) obtained the incorrect asymptotic result $J \sim r^{-(n+1)}$.

An improved asymptotic form can be obtained by setting $f = 1$ in (2.9):

$$\frac{d}{dr}(r^2 J) = -k(r) H_0. \tag{2.16}$$

For $R = \infty$, we may integrate this using (2.15) as a boundary condition as $r \to \infty$ to obtain

$$J \sim H_0 r^{-2} \left[1 + \int_r^\infty dr k(r)\right], \quad (R = \infty) \tag{2.17}$$

which, for power-law opacities, becomes

$$J \sim H_0 r^{-2} \left[1 + \frac{1}{n-1} r^{-(n-1)}\right], \quad (R = \infty). \tag{2.18}$$

It is clear from these results that the quantities $\mathscr{J} \equiv r^2 J, \mathscr{K} \equiv r^2 K$ and $\mathscr{H} \equiv r^2 H$ ($= H_0$ for the conservative case), are more natural variables for spherical problems than the moments themselves and, as will be seen shortly, satisfy simpler equations.

In terms of the optical depth from the surface ($r = R$),

$$\tau(r, R) \equiv \int_r^R k(r)\, dr, \tag{2.19}$$

which for power-law opacities becomes

$$\tau(r, R) = \frac{1}{n-1}\left[r^{-(n-1)} - R^{-(n-1)}\right], \tag{2.20}$$

the asymptotic results (2.12) and (2.18) may be written as

$$\mathscr{J} \cong 3H_0 \left(\frac{n-1}{n+1}\right)[\tau + \text{const.}], \quad (\text{large } \tau) \tag{2.21}$$

and

$$\mathscr{J} \cong H_0(1+\tau), \quad (\text{small } \tau). \tag{2.22}$$

Note that (2.21) is true for power-law opacities while (2.22) is true in general (for sufficiently large R). It is interesting that $\mathscr{J}$, and *not* J, behaves analogously with the source function to the plane-parallel Milne problem because of the geometrical dilution of the radiation in the spherical case.

By superposing the first terms in (2.21) and (2.22) to minimize the deviation of r^2H from H_0 Chapman constructed his approximate solution for the case $n = 3$ and $R = \infty$. Another such combination, which has been derived by simple but different arguments by Larson (1969) and by Rybicki (1971 to be published), is

$$\mathscr{J} \cong 3H_0 \left(\frac{n-1}{n+1}\right)\left[\tau+\frac{1}{3}\left(\frac{n+1}{n-1}\right)\right], \tag{2.23}$$

and will be compared to our accurate numerical results in Section 4.

2.1 *The limit* $R \ll 1$

In this case, the discussion of the approximate solution (2.12) can be carried further to elucidate the qualitative behaviour of the numerical solutions and to illustrate a fundamental difference between the transfer process in spherical and plane-parallel geometries.

In general f differs substantially from 1/3 only within a few units of optical depth from the outer boundary. When $R \leqslant 1$, the geometrical thickness of this region is very small compared to R and, in any event, f does not differ much from 1/3, even at the outer boundary. For example, for $n = 3$ and $R = 0{\cdot}1$, $\tau = 1$ occurs at $r = 0{\cdot}099$.

Replacing r in (2.12) by τ, using (2.20), and evaluating the constant of integration from the surface value of $\mathscr{J}$, which we parameterize as

$$\mathscr{J}(R) = \lambda\mathscr{H}(R) = \lambda H_0, \tag{2.24}$$

we obtain

$$\mathscr{J} = 3\left(\frac{n-1}{n+1}\right) H_0[\tau+Q_n(\tau)], \tag{2.25}$$

where

$$Q_n(\tau) = R^{-(n-1)}+[\tau+R^{-(n-1)}]^{-2/(n-1)}\left[\frac{1}{3}\left(\frac{n+1}{n-1}\right)\lambda-R^{-(n-1)}\right]R^{-2} \tag{2.26}$$

is a spherical analogue of the Hopf q-function. From the near-isotropy of the emergent radiation, we expect

$$\lambda \lesssim \sqrt{3} \tag{2.27}$$

for sufficiently small R. From (2.26) we observe that $Q_n(\tau)$ goes from negative to positive as τ increases from zero and approaches its asymptotic value algebraically, rather than exponentially through positive values as does the Hopf q-function. Finally as $\tau \to \infty$, $Q_n \to R^{-(n-1)}$. All of these features are consequences of spherical symmetry and are not artifacts induced by the Eddington approximation. The results of this section will be compared with the numerical results in Section 4.

2.2 *The iteration procedure*

Given an initial estimate of the Eddington factor $f(r)$ and of the Eddington 'boundary factor'

$$g \equiv H(R)/J(R), \tag{2.28}$$

we can numerically integrate the moment equation (2.9) to obtain an estimate of $J(r)$, say $J^0(r)$. In the second half of the iteration cycle we evaluate the solution of (2.1) in which $J(r)$ is replaced by the known function $J^0(r)$, thereby determining an estimate of $I(r, \mu)$, its moments and finally new estimates of $f(r)$ and g. The process is repeated until the desired degree of convergence is obtained. For opacity laws such that large optical depths occur at small radii, no special assumptions need be made concerning the behaviour of $J(r)$ or $f(r)$; the latter converges automatically to 1/3. It should be noted that no special properties of $k(r)$ are assumed in this method. Our choice of power-law opacities is guided by convenience in exposition and by the historical development of this problem.

2.21 *Integration of the moment equation.* A natural variable to use in the numerical integration of (2.9) is

$$y(r) \equiv f(r)r^2J(r), \tag{2.29}$$

which satisfies the equations

$$y'(r)+\frac{1}{r}[1+1/f]y(r)+H_0k(r) = 0 \tag{2.30}$$

and

$$y(R) = H_0f(R)/g. \tag{2.31}$$

The inward integration starting from $r = R$ to some deep interior point $r = r_{\min}$ is stable and readily performed numerically. Although in this calculation a version of the integration procedure described by Bulirsch & Stoer (1966) is used, it appears that most other commonly used procedures should also be effective. The radius $r = r_{\min}$ at which the integration is terminated is arbitrary, subject to the condition that the radiation field at that point be highly isotropic. In practice r_0 was chosen to lie below $\tau = 100$.

2.22 *Formal solution.* There are, of course, integral expressions for $I(r, \mu)$ and its moments if $J(r)$ in (2.1) is assumed known. The evaluation of these expressions is discussed by Chapman (1966) for power-law opacities. It is more efficient, however, to evaluate the formal solution numerically through the solution of difference equations by means of a technique introduced into radiative transfer calculations by Feautrier (1964a).

In order to use Feautrier's technique conveniently and also to treat accurately the outward peaking of the radiation field, we introduce the (p, z) representation. By eliminating θ through the relation

$$p \equiv r \sin\theta \tag{2.32}$$

and using p and either r or

$$z \equiv \sqrt{r^2-p^2}, \tag{2.33}$$

as convenient, for the other coordinate, (cf. Fig. 1), we can rewrite the transfer equation as

$$\frac{\partial I^{\pm}}{\partial z}(p, z) = \pm k(r)[J(r)-I^{\pm}(p, z)], \tag{2.34}$$

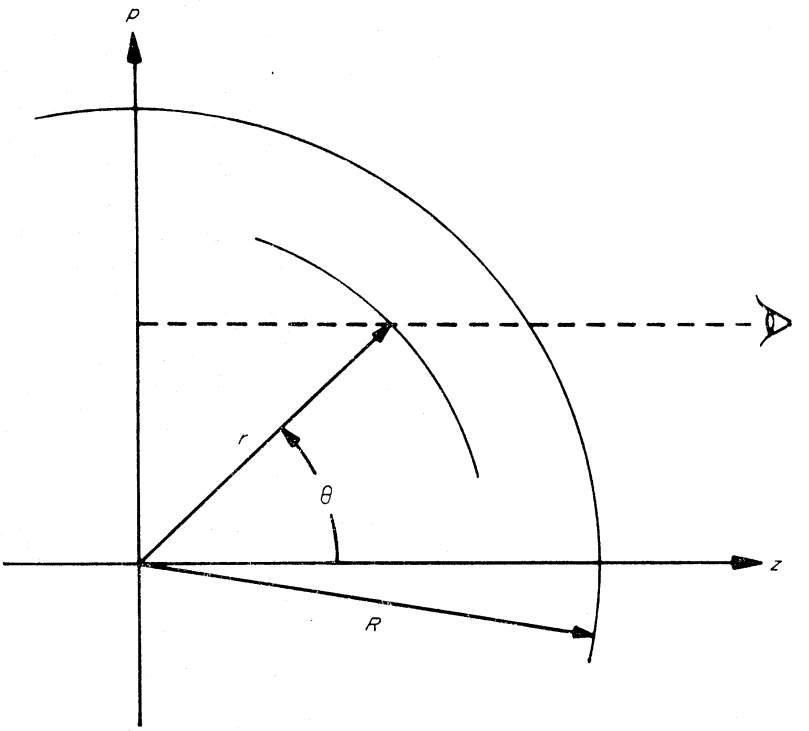

FIG. 1. *The coordinate systems* (r, θ) *and* (p, z).

where I^+ and I^- refer to the radiation flowing to the right and to the left along the dashed line in Fig. 1. Since $k(r)$ and $J(r)$ depend on p and z only through the combination $\sqrt{p^2+z^2}$, we continue to write r as the argument of these functions. The boundary conditions are

$$I^+(p, z) = I^-(p, z), \quad z = 0 \tag{2.35}$$

and

$$I^-(p, z) = 0, \quad z = z_{\max}(p) \equiv \sqrt{R^2-p^2}. \tag{2.36}$$

In terms of the quantities

$$u(p, z) \equiv \tfrac{1}{2}[I^+(p, z)+I^-(p, z)] \tag{2.37}$$

and

$$v(p, z) \equiv \tfrac{1}{2}[I^+(p, z)-I^-(p, z)], \tag{2.38}$$

the moment integrals become

$$J(r) = \frac{1}{r}\int_0^r dpp(r^2-p^2)^{-1/2}u(p, r) \tag{2.39}$$

$$H(r) = \frac{1}{r^2}\int_0^r dppv(p, r) \tag{2.40}$$

$$K(r) = \frac{1}{r^3}\int_0^r dpp(r^2-p^2)^{1/2}u(p, r). \tag{2.41}$$

In terms of the quantities $u(p, z)$ and $v(p, z)$ defined in (2.37) and (2.38), the transfer equation may be expressed as

$$\frac{1}{k(r)}\frac{\partial u(p,z)}{\partial z} = -v(p,z) \tag{2.42}$$

and

$$\frac{1}{k(r)}\frac{\partial v(p,z)}{\partial z} = u(p,z)+J(r). \tag{2.43}$$

Eliminating $v(p, z)$ we obtain

$$\frac{1}{k(r)}\frac{\partial}{\partial z}\left[\frac{1}{k(r)}\frac{\partial u(p,z)}{\partial z}\right] = u(p,z)-J(r), \tag{2.44}$$

with the boundary conditions

$$\frac{1}{k(r)}\frac{\partial u(p,z)}{\partial z} = 0, \quad z = 0 \tag{2.45}$$

$$\frac{1}{k(R)}\frac{\partial u(p,z)}{\partial z}+u(p,z) = 0, \quad z = \sqrt{R^2-p^2}. \tag{2.46}$$

2.23 *The difference equations.* For each value of p, (2.44) is to be integrated from $z = 0$ to $z = \sqrt{R^2-p^2}$. To this end we propose a difference scheme involving the z-points $z_1 = 0, z_2, z_3, \ldots z_Q = \sqrt{R^2-p^2}$. By defining

$$f_\beta \equiv \tfrac{1}{2}(k_{\beta+1}+k_\beta)(z_{\beta+1}-z_\beta), \quad \beta = 1, 2, \ldots Q-1 \tag{2.47}$$

where k_β is the value of $k(r)$ at $r = \sqrt{p^2+z_\beta^2}$, we can write the approximate differentiation formula (suppressing the argument p)

$$\frac{1}{k(r)}\frac{\partial}{\partial z}\left(\frac{1}{k(r)}\frac{\partial u(r)}{\partial z}\right)\Bigg|_\beta \cong 2\left[u_{\beta+1}\frac{1}{f_\beta}-u_\beta\left(\frac{1}{f_\beta}+\frac{1}{f_{\beta-1}}\right)+u_{\beta-1}\frac{1}{f_{\beta-1}}\right](f_\beta+f_{\beta-1}). \tag{2.48}$$

To incorporate the boundary conditions and to obtain $v(p, z)$, in the manner discussed by Auer (1967), we use the Taylor expansion of u about $z = z_\beta$ written in the form

$$u_{\beta+1} = u_\beta+\frac{1}{k_\beta}\frac{\partial u}{\partial z}\Bigg|_\beta f_\beta+\frac{1}{2}\frac{1}{k_\beta}\frac{\partial}{\partial z}\left[\frac{1}{k_\beta}\frac{\partial u}{\partial z}\right]\Bigg|_\beta f_\beta{}^2 + \frac{1}{6}\frac{1}{k_\beta}\frac{\partial}{\partial z}\left[\frac{1}{k_\beta}\frac{\partial}{\partial z}\left(\frac{1}{k_\beta}\frac{\partial u}{\partial z}\right)\right]\Bigg|_\beta f_\beta{}^3+\ldots. \tag{2.49}$$

It is not necessary to retain the third-order term in (2.49), but it may be readily evaluated in terms of $(1/r)(dJ/dr)$ which is easily obtained during the integration of the moment equation and its retention appears to substantially increase the accuracy with which $v(p, z)$ can be obtained. Using (2.42)–(2.46) and (2.49), we find for the boundary conditions on $u(z_\beta)$ and the values of $v(z_\beta)$ the following relations:

$$u_1[1+\tfrac{1}{2}f_1{}^2]-u_2 = \tfrac{1}{2}f_1{}^2J_1 \tag{2.50}$$

$$u_{Q-1}-u_Q[1+f_{Q-1}+\tfrac{1}{2}f_{Q-1}{}^2+\tfrac{1}{6}f_{Q-1}{}^3] = -\tfrac{1}{2}f_Q{}^2J_Q+\tfrac{1}{6}f_Q{}^3\frac{1}{k_Q}\frac{z_Q}{r_Q}\frac{dJ}{dr}\Bigg|_Q \tag{2.51}$$

$$v_\beta = \left\{-u_{\beta+1}+u_\beta[1+\tfrac{1}{2}f_\beta{}^2]-\tfrac{1}{2}f_\beta{}^2J_\beta-\tfrac{1}{6}f_\beta{}^3\frac{1}{k_\beta}\frac{z_\beta}{r_\beta}\frac{dJ}{dr}\Bigg|_\beta\right\}\Big/[f_\beta+\tfrac{1}{6}f_\beta{}^3], \quad \beta = 2, 3, \ldots Q-1. \tag{2.52}$$

In writing (2.49) we used the fact that $dJ/dz = 0$ at $z = 0$. Since (2.48), (2.50) and (2.51) have the form

$$-A_\beta u_{\beta-1}+B_\beta u_\beta - C_\beta u_{\beta+1} = L_\beta, \quad \beta = 1, 2, \ldots Q, \tag{2.53}$$

we can solve for $\{u_\beta\}$ by the scheme

$$D_1 = C_1/B_1, \quad \nu_1 = L_1/B_1 \tag{2.54}$$

$$D_\beta = C_\beta/(B_\beta - A_\beta D_{\beta-1}), \quad \nu_\beta = (L_\beta + A_\beta \nu_{\beta-1})/(B_\beta - A_\beta D_{\beta-1}), \quad \beta = 2, 3, \ldots Q, \tag{2.55}$$

$$u_{Q+1} = 0 \tag{2.56}$$

$$u_\beta = \nu_\beta + D_\beta u_{\beta+1}, \quad \beta = Q, Q-1, \ldots 1. \tag{2.57}$$

Once $\{u_\beta\}$ are known, $\{v_\beta\}$ can be obtained from (2.57) augmented by the values

$$v_1 = 0, \quad v_Q = u_Q, \tag{2.58}$$

which follow from (2.45) and (2.46) respectively.

2.24 *Evaluation of the moment integrals.* Evaluation of the integrals (2.39) and (2.41) is seriously complicated by the factors $(r^2-p^2)^{\pm 1/2}$. For this reason piecewise quadratic fits to $u(p, r)$ and $v(p, r)$ are formed, in terms of which the integrations may readily be performed analytically. As it is not feasible to continue the integration of the moment equation to its singular point at $r = 0$, a minimum non-zero value of r is used equal to the smallest value of p. No attempt is made to evaluate the moment integrals at this point on the basis of the one available value of u and v, as f at this point is easily obtained by inward extrapolation and in any event differs only minutely from 1/3.

At each value of r larger than the minimum, the value of $u(p = 0, r)$ is estimated from the known values at the two smallest values of p, using an expression of the form

$$u(p) = u(0)+ap^2, \tag{2.59}$$

which reflects the fact that $u(p)$ is an even function; $v(0)$ is estimated similarly. Although this procedure is quite satisfactory for $u(p)$, which varies quite slowly near $p = 0$, it is less accurate for $v(p)$. These expressions for u and v are used to evaluate the contribution to the moment integrals from $p = 0$ to the first discrete p-value, and the piecewise quadratic fits to continue the integration to $p = r$.

3. COMPUTATIONAL ASPECTS

In implementing the above analysis, several more or less subjective judgments had to be made. These will be discussed here, along with the checks that could be made on the accuracy of the solutions.

3.1 *Discretization*

The choice of r- and p-points is subject to several considerations. Integration of the transfer equation requires a rather fine mesh of r-points, while the moment integrals can be evaluated on a rather coarser distribution of p-points. It is also

necessary that each integration of the transfer equation start at $z = 0$, that is, at $r = p$. Thus the p-mesh $\{p_i, i = 1, 2, \ldots n\}$ was chosen as a subset of the r-mesh $\{r_j, j = 1, 2, \ldots m\}$, subject to the requirements that $p_1 = r_1$ and $p_n = r_m \equiv R$, $m \geqslant n$. If we define $k(i)$ to be the ordinal number of the r-point equal to p_i, that is, $r_{k(i)} \equiv p_i$, then the z-points used in integrating the transfer equation at a fixed value $p = p_i$, are

$$z_j = \sqrt{r_{j-1+k(i)}{}^2 - p_i{}^2}, \quad j = 1, 2, \ldots Q \equiv m + 1 - k(i). \tag{3.1}$$

An approximately logarithmic distribution of the p-points appears to be satisfactory. The rapid variation of $v(p)$ for small values of r causes $H(r)$ to be evaluated less accurately than $J(r)$ and $K(r)$ for small values of r, but because $H(r)$ enters the calculation only at $r = R$, this loss of accuracy is unimportant.

An approximately logarithmic distribution of the r-points is also satisfactory except that extra points must be used for $r \sim R$ in order to cope with the rapid change in the radiation field with radius near the surface. In practice the p-points were specified along with the number of r-points to be inserted between each p-point. Typically, for $R = 3$, about 50 p-points and 200 r-points were used. No attempt has been made to optimize the mesh, since at present the main interest is in obtaining accurate solutions to use as standards. However, it now appears that the number of p-points can be cut significantly.

The moment integrals and hence $f(r)$ can be evaluated only at those r-points equal to p-points, but $f(r)$ is required at all r-points in the solution of the moment equation. Cubic Lagrange interpolation proved adequate to provide $f(r)$ at the intermediate points.

3.2 *Convergence*

The rate of convergence was quite remarkable. Starting with an initial estimate

$$f(r) = 1 - \tfrac{2}{3} e^{-\beta r},$$

where β is the inverse of the radius at which optical depth unity occurred, essentially complete convergence was achieved in three iterations, although for all results given in this paper, a fourth iteration was performed as a check. In Table I we show typical values of $J(r)$, $f(r)$ and g for $R = 10$, $N = 2$ after each of four iterations.

3.3 *Accuracy of solutions*

All solutions obtained satisfy the obvious physical requirements that: (1) $f(r)$ is a monotonically increasing, and $\mathcal{J}(r)$ a monotonically decreasing, function of r, for each value of R; (2) if $R_2 > R_1$, then $\mathcal{J}(r, R_1) < \mathcal{J}(r, R_2)$ and $f(r, R_1) < f(r, R_2)$, $r \leqslant R_1$. Our solution for $R = 10$, $N = 3$ satisfies these criteria with regard to Schmid-Burgk's (1971) solution for $R = \infty$ and is in good agreement with his solution below a few optical depths, as one would expect. At optical depths of 100 or more, the numerical values of $r^2 J$ agree with the asymptotic expression (2.12) to better than three significant figures and f differs from 1/3 in the fifth or sixth place. In cases when R is large, $\mathcal{J}$ approaches H_0 in reasonable accord with the asymptotic result (2.18), especially for $N = 3$ when the 'missing optical depth' between $R = 10$ and $R = \infty$ is $\Delta\tau = 0{\cdot}005$.

In all cases the total flux $\mathcal{H}$, as obtained by evaluating (2.40) as described above,

TABLE I

Iteration history for $N = 2$, $R = 10$

r	(0) $f(r)$	(1) $J(r)$	(1) $f(r)$	(2) $J(r)$	(2) $f(r)$	(3) $J(r)$	(3) $f(r)$	(4) $J(r)$	(4) $f(r)$
0·04	0·3620	1·643+4	0·3345	1·572+4	0·3345	1·573+4	0·3345	1·573+4	0·3345
0·10	0·4028	1·159+3	0·3403	1·031+3	0·3408	1·035+3	0·3408	1·035+3	0·3408
0·40	0·5706	2·846+1	0·4001	1·995+1	0·4091	2·010+1	0·4094	2·012+1	0·4094
1·00	0·7781	2·877	0·5317	1·883	0·5415	1·884	0·5425	1·884	0·5427
2·00	0·9261	5·533−1	0·6684	3·612−1	0·6729	3·615−1	0·6731	3·614−1	0·6732
4·00	0·9918	1·169−1	0·7901	7·630−2	0·7927	7·637−2	0·7928	7·637−2	0·7928
6·00	0·9991	4·856−2	0·8485	3·163−2	0·8516	3·165−2	0·8517	3·165−2	0·8517
8·00	1·000	2·614−2	0·8876	1·700−2	0·8909	1·701−2	0·8910	1·701−2	0·8910
9·00	1·0000	2·024−2	0·9053	1·316−2	0·9084	1·317−2	0·9085	1·317−2	0·9085
9·50	1·0000	1·796−2	0·9148	1·168−2	0·9178	1·169−2	0·9178	1·169−2	0·9178
10·00	1·0000	1·598−2	0·9270	1·040−2	0·9294	1·040−2	0·9296	1·040−2	0·9296
g	0·5774		0·9568		0·9584		0·9584		0·9584

differs from H_0 by less than 1 per cent, except at small radii where the evaluation of that integral is inaccurate. In such cases, the reduction in r and p intervals for small values improves the values of $\mathscr{H}$ without altering J and f, so that the apparent flux error in the small-r region is inconsequential. The flux is also monitored by substituting J and K into (2.7) and solving for H. This involves numerical differentiation of K, but in regions when this can be done with confidence, the flux error is again less than 1 per cent.

Finally, an estimate of the numerical accuracy can be found by repeating the calculation using finer r and p meshes. This leads to the conclusion that $J(r)$ and $f(r)$ are everywhere accurate to a few tenths of a per cent except at the boundary $r = R$, where the error may be as large as 1 per cent.

3.4 *Timing*

The times required for four iterations using on the order of 60 p-points and 200 r-points on the CDC 6400 was approximately 100 s. This is too long for the method as it now stands to be applied to non-grey and particularly non-LTE spherical model atmospheres. However, no attempt has been made to optimize either the coding or the choice of mesh points and of course a 25 per cent reduction is available immediately by reducing the number of iterations to three. Also most practical work would probably not require the high accuracy obtained here, so that fewer depths and values of p could be used. Work is in hand to develop a more efficient program and it is expected that times on the order of 10 s are quite feasible, programming in FORTRAN, and even less if certain parts of the program are coded in assembly language. For non-grey problems the increase in time with the number of frequencies should be less than linear because many of the housekeeping aspects of the program need not be repeated for each frequency.

4. NUMERICAL RESULTS

Computations have been carried out for $n = 3/2$, 2 and 3 using a number of values of $R \geqslant 0{\cdot}1$, with $H_0 = 1$. In Figs 2, 3 and 4 $\mathscr{J}(r)$ and $f(r)$ are plotted for the indicated values of R. In these figures the asymptotic form

$$\mathscr{J}_{\text{asymp}}(r) = 3r^{-(n-1)}/(n+1) \qquad (4.1)$$

and the limiting value of $\mathcal{J}(r) = H_0 = 1$ are represented by dashed lines. In the top panels of these figures the Eddington factors $f(r)$ and g appear; the vertical arrows indicate the radius at which optical depth unity occurs for each value of R.

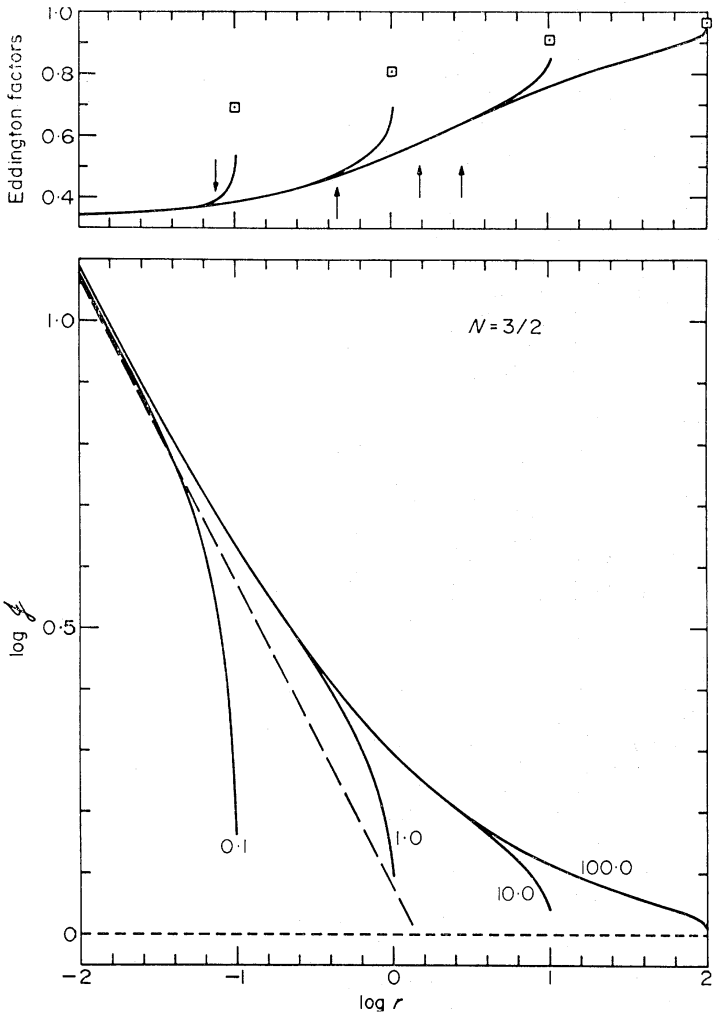

FIG. 2. $\mathcal{J}(r)$, $f(r)$ vs. *radius and* $g(R)$ *for* $n = 3/2$ *and the indicated values of* R. *The long dashes represent* $\mathcal{J}_{\text{asymp}}$ *and the vertical arrows indicate the radius at which* $\tau = 1$ *occurs for each* R.

For the smallest values of R shown in the figures, $\mathcal{J}$ departs from $\mathcal{J}_{\text{asymp}}$ according to the discussion in Section 2.1. In Table II accurate numerical values of $\mathcal{J}(r)$ for $R = 0{\cdot}1$ and all three values of n are given along with the ratio of the result given by equation (2.25) to the accurate numerical result, for both $\lambda = \sqrt{3}$ and $\lambda = \mathcal{J}(R)$ as calculated. Except at the outer-most points, the results using $\lambda = \sqrt{3}$ are superior.

For R of the order of unity, we see that $\mathcal{J}(r)$ rises above $\mathcal{J}_{\text{asymp}}$ and then falls at the boundary, and for $R \gg 1$, $\mathcal{J}(r)$ lies above $\mathcal{J}_{\text{asymp}}$ right to the boundary and in fact forms an extensive region in which it varies quite slowly. It is in this latter region that the radiation field is becoming strongly outward-peaked and is presumably of most interest in connection with stars with extensive atmospheres. We can refer to the region in which $\mathcal{J} \simeq \mathcal{J}_{\text{asymp}}$ as the *diffusion* region and that in which $\mathcal{J} \gg \mathcal{J}_{\text{asymp}}$ as the *geometrical* region. In the latter region $\mathcal{J}(r)$ varies appreciably

TABLE II

Comparison of equation (2.25) with computed values of $\mathcal{J}$ for $R = 0{\cdot}1$

		$n = 3/2$			$n = 2$			$n = 3$	
		$\mathcal{J}(\lambda = \sqrt{3})$	$\mathcal{J}(\lambda = 1{\cdot}448)$		$\mathcal{J}(\lambda = \sqrt{3})$	$\mathcal{J}(\lambda = 1{\cdot}593)$		$\mathcal{J}(\lambda = \sqrt{3})$	$\mathcal{J}(\lambda = 1{\cdot}644)$
r	$\mathcal{J}_{\text{num}}$	$\mathcal{J}_{\text{num}}$	$\mathcal{J}_{\text{num}}$	$\mathcal{J}_{\text{num}}$	$\mathcal{J}_{\text{num}}$	$\mathcal{J}_{\text{num}}$	$\mathcal{J}_{\text{num}}$	$\mathcal{J}_{\text{num}}$	$\mathcal{J}_{\text{num}}$
0·010	12·20	0·98	0·98	99·97	1·00	1·00	7499·0	1·00	1·00
0·030	7·039	0·96	0·95	32·71	1·00	1·00	826·8	1·00	1·00
0·050	5·133	0·95	0·93	18·11	0·99	0·99	281·8	1·00	1·00
0·070	3·726	0·95	0·91	10·46	0·98	0·97	117·4	1·00	1·00
0·090	2·350	0·99	0·89	4·639	0·95	0·93	33·57	0·99	0·99
0·095	1·961	1·04	0·90	3·247	0·94	0·91	17·34	0·98	0·97
0·097	1·788	1·07	0·92	2·667	0·95	0·90	11·14	0·97	0·96
0·098	1·694	1·09	0·93	2·362	0·96	0·90	8·098	0·95	0·94
0·099	1·591	1·13	0·95	2·033	0·98	0·92	5·069	0·93	0·91
0·100	1·448	1·20	1·00	1·593	1·09	1·00	1·644	1·05	1·00

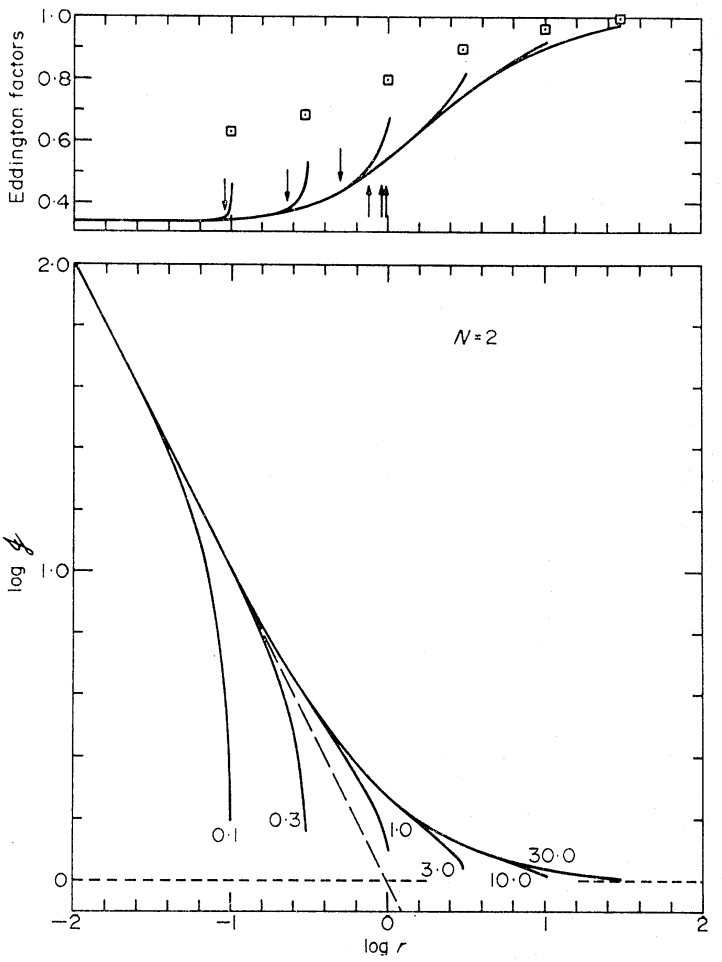

FIG. 3. $\mathcal{J}(r)$, $f(r)$ vs. *radius and* $g(R)$ *for* $n = 2$ *and the indicated values of* R. *The long dashes represent* $\mathcal{J}_{\text{asymp}}$ *and the vertical arrows indicate the radius at which* $\tau = 1$ *occurs for each* R.

only when r changes by its own magnitude, while in the diffusion region $\mathcal{J}$ varies over a mean free path. If R is not too large, a third region is discernable for $r \approx R$ in which the decrease in $\mathcal{J}$ and the increase in f become more rapid. Both the direction and approximate magnitude of these deviations from the infinite-atmosphere asymptotic results may be regarded as arising from the removal of the region for which $r > R$ and are seen to be in accord with our experience in plane-parallel atmospheres.

In Table III the cases with the largest value of R for each n are compared with the approximate expression (2.23) using both $R = \infty$ and the value used in obtaining the numerical result. The two sets of approximate values differ by a constant and the maximum errors for both choices of R are given. The maximum errors occur in all cases at $r \sim 0{\cdot}3$.

The Eddington factor $f(r)$ is plotted *vs.* τ in Fig. 5 for $n = 2$ and $R = 0{\cdot}1$, $1{\cdot}0$ and $10{\cdot}0$, along with the results for $R = 1{\cdot}0$ and $n = 3/2$ and 3 for comparison. It is clear that most of the variation in $f(r)$ occurs within the first optical depth, although a substantial part of the departure of f from $1/3$, especially in an extensive region for which $\tau > 1$, is a direct consequence of the spherical geometry.

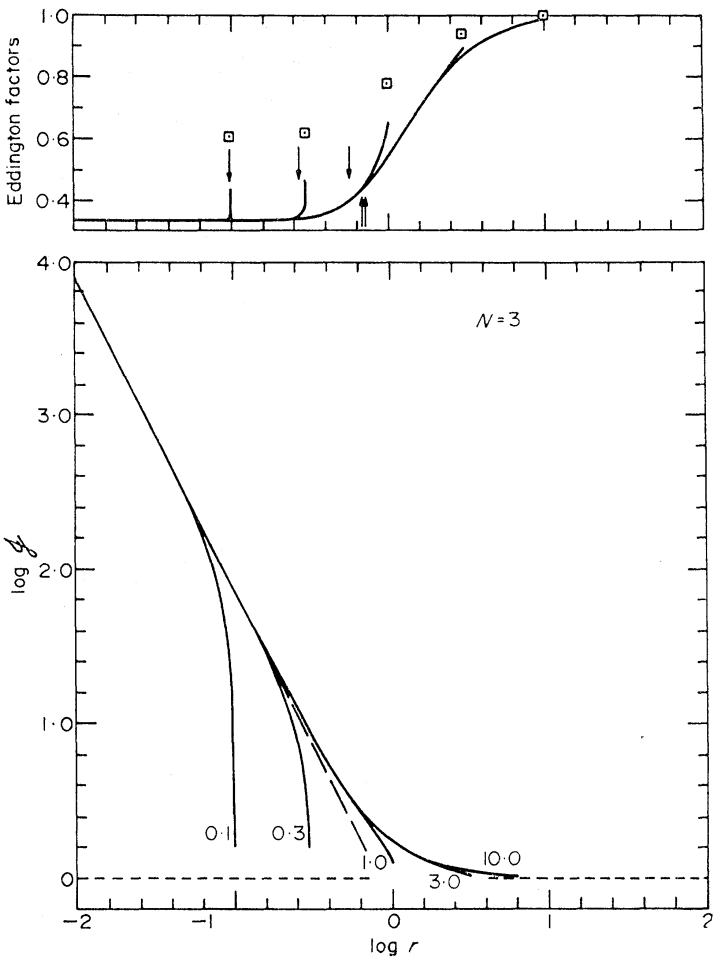

FIG. 4. $\mathcal{J}(r)$, $f(r)$ vs. *radius and* $g(R)$ *for* $n = 3$ *and the indicated values of* R. *The long dashes represent* $\mathcal{J}_{\text{asymp}}$ *and the vertical arrows indicate the radius at which* $\tau = 1$ *occurs for each* R.

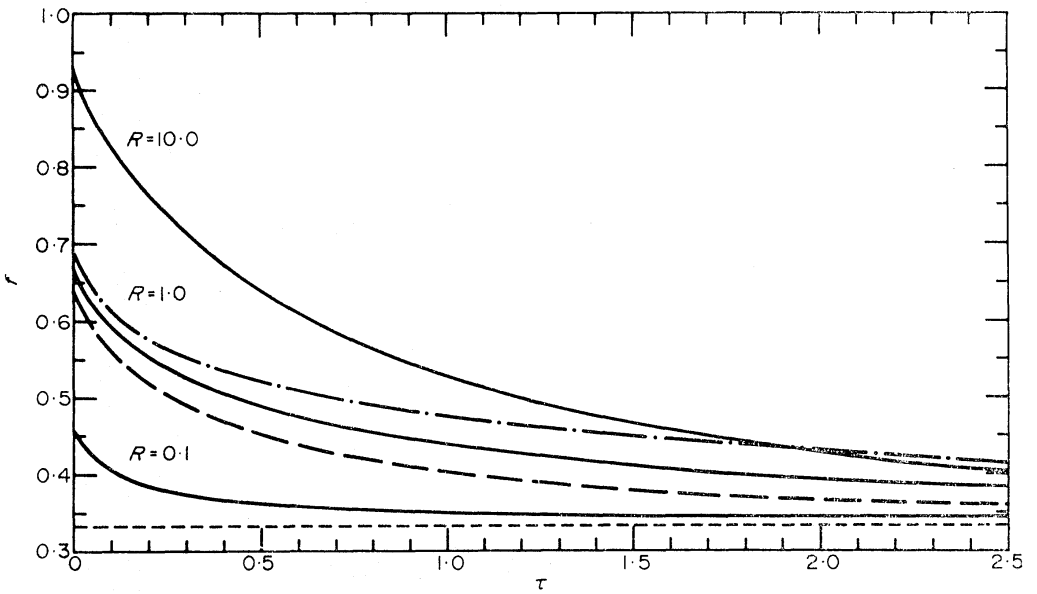

FIG. 5. *The Eddington factor* f vs. *optical depth for* $n = 2$ *and the indicated values of* R. *Also shown are results for* $n = 3/2$ (–·–·–·–·–) *and* $p = 3$ (———).

TABLE III

Comparison of equation (2.23) with numerical results

	$n = 3/2$		$n = 2$		$n = 3$	
τ	$\mathcal{J}_{\text{approx}}^{(R=\infty)}$	$\mathcal{J}_{\text{num}}^{(R=100)}$	$\mathcal{J}_{\text{approx}}^{(R=\infty)}$	$\mathcal{J}_{\text{num}}^{(R=30)}$	$\mathcal{J}_{\text{approx}}^{(R=\infty)}$	$\mathcal{J}_{\text{num}}^{(R=10)}$
0·03	7·93	7·28	34·3	33·5	834·0	833·0
0·10	4·79	4·29	11·0	10·4	76·0	75·1
0·30	3·19	2·83	4·33	3·9	9·33	8·93
1·00	2·20	1·98	2·00	1·88	1·75	1·78
3·00	1·69	1·55	1·33	1·30	1·08	1·11
10·0	1·38	1·30	1·10	1·09	1·008	1·006
30·0	1·22	1·17	1·03	1·01		
100·0	1·12	1·03				
Finite R correction	−0·120		−0·033		−0·008	
Max error ($R = \infty$)		13%		9%		5%
Max error (R finite)		9%		8%		5%

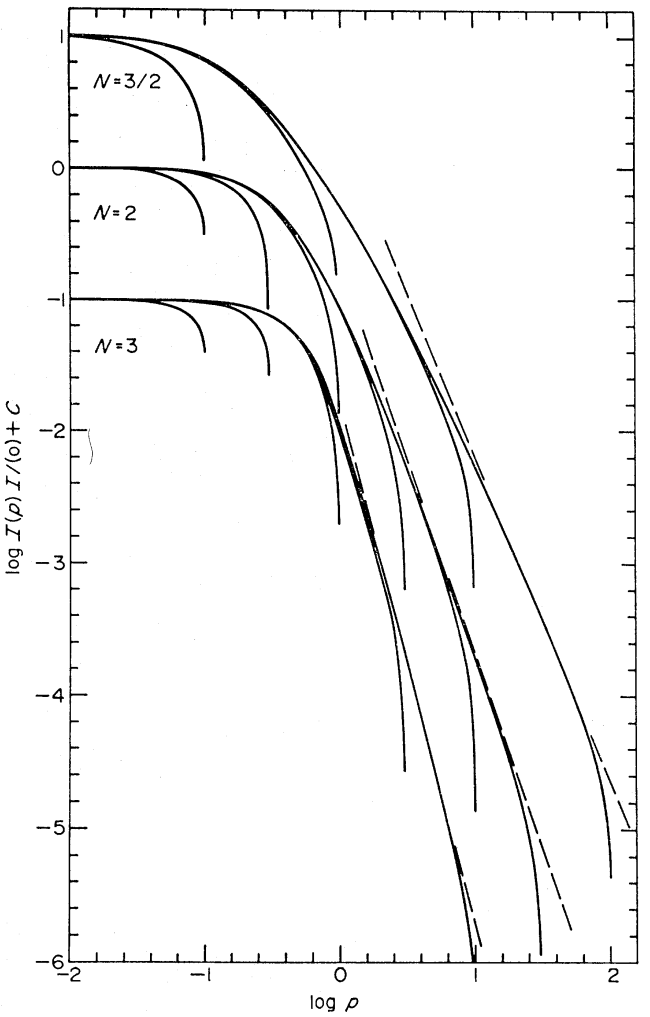

FIG. 6. *The limb-darkening curves $I(p)/I(0)$ vs. p. The curves for $n = 3/2$ and $n = 3$ have been displaced upwards and downwards, respectively, by a decade. The dashed lines represent the asymptotic results for $R = \infty$.*

TABLE IV

Disk centre intensities $I(p = 0)$

R	$n = 3/2$	$n = 2$	$n = 3$
0·1	8·20+2	5·61+2	5·06+2
0·3		8·19+1	6·11+1
1·0	3·82+1	1·89+1	1·19+1
3·0		1·03+1	8·18
10·0	1·01+1	8·18	7·78
30·0		7·65	
100·0	6·57		

4.1 *Emergent intensity*

The limb-darkening functions $I(p)/I(0)$ are plotted as a function of p in Fig. 6. The curves for $n = 3/2$ have been displaced upwards by a decade, and those for $n = 3$, downwards by the same amount. The values of $I(0)$ are given in Table IV. It is clear that as n increases, the decrease in $I(p)$ and p becomes more abrupt, approaching the uniform disk model.

For those values of p for which the tangential optical depth

$$\tau_t(p) = 2\int_0^{\sqrt{R^2-p^2}} dzk(\sqrt{p^2+z^2}) \tag{4.2}$$

is much less than unity, the emergent intensity is simply

$$I(p) \simeq 2\int_0^{\sqrt{R^2-p^2}} dzk(\sqrt{p^2+z^2})J(\sqrt{p^2+z^2}). \tag{4.3}$$

For $R = \infty$, we can use the approximate limiting result $J = H_0 r^{-2}$, to obtain for power-law opacities,

$$I(p) \sim C_n p^{-(n+1)} \ (R = \infty). \tag{4.4}$$

For $n = 2$ and 3, $C_2 = \pi/2$ and $C_3 = 4/3$. Chandrasekhar (1935) obtained the incorrect result $I(p) \sim p^{-2n}$.

The result (4.4) is represented on Fig. 6 by broken lines. For $n = 2$ and 3, the known values of the constant C_n were used, while for $n = 3/2$, the constant was chosen to make the asymptotic curve lie tangent to the $R = 100$ case.

4.2 *Further developments*

Applications of the method developed in this paper to spherical problems with non-conservative scattering, non-grey opacities and polarized radiation are now underway and will be reported shortly.

ACKNOWLEDGMENT

We are grateful to David van Blerkom and John Castor for the benefit of their experience in using the p–z representation, and to Dr Castor for subsequent helpful discussions. We are also deeply indebted to Mrs Chela Kunasz for her unfailing and enthusiastic assistance in preparing and testing the computer program. Dr Johannes Schmid-Burgk has been so kind as to give us his results for $n = 3$ in advance of publication. This research was supported by the Advanced Research Projects Agency, Department of Defense, and was monitored by U.S. Army Research Office—Durham, under Contract No. DA-31-124-ARO-D-139.

The work reported here was performed while G. B. Rybicki was a Visiting Fellow of the Joint Institute for Laboratory Astrophysics.

D. G. Hummer:
Joint Institute for Laboratory Astrophysics, National Bureau of Standards and University of Colorado, Boulder, Colorado 80302

G. B. Rybicki:
Smithsonian Astrophysical Observatory, Cambridge, Massachusetts, 02138

REFERENCES

Auer, L., 1967. *Astrophys. J.*, **150**, L53.
Auer, L. H. & Mihalas, D., 1970. *Mon. Not. R. astr. Soc.*, **149**, 65.
Böhm-Vitense, E., 1963. *Z. Astrophys.*, **57**, 241.
Bulirsch, R. & Stoer, J., 1966. *Numerische Mathematik*, **8**, 1.
Carlson, B. G. & Lathrop, K. D., 1968. In *Computing Methods in Reactor Physics*, eds H. Greenspan, C. N. Kelber and D. Okrent, Gordon and Breach, New York.
Cassinelli, J. P., 1971. *Astrophys. J.*, **165**, in press.

Castor, J. I., 1970. *Mon. Not. R. astr. Soc.*, **149,** 111.
Chandrasekhar, S., 1934a. *Mon. Not. R. astr. Soc.*, **94,** 444.
Chandrasekhar, S., 1934b. *Astr. Zh.*, **11,** 550.
Chandrasekhar, S., 1935. *Proc. Camb. Phil. Soc.*, **31,** 390.
Chandrasekhar, S., 1945. *Astrophys. J.*, **101,** 95.
Chapman, R. D., 1966. *Astrophys. J.*, **143,** 61.
Eddington, A. S., 1926. *The Internal Constitution of the Stars*, Cambridge University Press.
Feautrier, P., 1964a. *C.r. hebd. Séanc. Acad. Sci. Paris*, **258,** 3189.
Feautrier, P., 1964b. In *Proceedings First Harvard–Smithsonian Conference on Stellar Atmospheres*, Special Report 167, Smithsonian Astrophysical Observatory, Cambridge, Mass, p. 108.
Larson, R. B., 1969. *Mon. Not. R. astr. Soc.*, **145,** 297.
Kosirev, N. A., 1934. *Mon. Not. R. astr. Soc.*, **94,** 430.
Pearce, W. P., 1967. Radiative Transfer in Finite Extended Stellar Atmospheres, Ph.D. Thesis, Northwestern University, Evanston, Illinois.
Pomraning, G. C., 1969. *J. quantit. Spectrosc. radiat. Transfer*, **9,** 407.
Wilson, S. J. & Sen, K. K., 1965a. *Ann. Astrophys.*, **28,** 348.
Wilson, S. J. & Sen, K. K., 1965b. *Ann. Astrophys.*, **28,** 855.
Woolley, R. v. d. R. & Stibbs, D. W. N., 1953. *The Outer Layers of a Star*, Oxford University Press.
Wrubel, M. H., 1949. *Astrophys. J.*, **110,** 288.